Environ Sci Pollut Res (2018) 25:1115–1131
https://doi.org/10.1007/s11356-017-0499-8

RESEARCH ARTICLE

Simulating and mapping the spatial and seasonal effects of future climate and land -use changes on ecosystem services in the Yanhe watershed, China

Dengshuai Chen [1,2] · Jing Li [1,2] · Zixiang Zhou [3] · Yan Liu [1,2] · Ting Li [1,2] · Jingya Liu [1,2]

Received: 18 July 2017 / Accepted: 16 October 2017 / Published online: 27 October 2017

Abstract Effective information about ecosystem services is essential to help optimize and prioritize activities that support conservation planning in the face of land use and climate changes. This study shows an approach that integrates several dissimilar models for assessing water-related ecosystem services to predict values in 2050 under three land use scenarios in the Yanhe watershed. The simulated output variables pertaining to water yield and sediment yield were used as indicators for two ecosystem-regulating services, i.e., water flow regulation and erosion regulation, which were quantified using the soil and water assessment tool (SWAT) model. The model results were translated into a relative ecosystem service valuation scale, which facilitated the analysis of spatial and seasonal changes and served as the basis for the applied mapping approach. The simulated results indicate that higher water-related regulation services were concentrated in the middle and lower reaches of rivers with high water yield and low sediment erosion. The highest water flow regulation services occurred in summer; nevertheless, this was when erosion regulation services were the lowest compared to other periods in 2050. A comparison of the three land use scenarios showed differences in the water-related regulation services. Scenario 1, with high forest coverage, had the highest erosion regulation services, but the water flow regulation services were the lowest. Scenario 3 showed the reverse pattern. Scenario 2 had intermediate water flow regulation and erosion regulation. Increasing vegetation cover in the watershed is conducive to controlling water and soil erosion but could lead to a decline in available water resources. Spatial mapping is a powerful tool for displaying the spatiotemporal differences in the water-related regulation services delivered by ecosystems and can help decision makers optimize land use in the future, with the goal of maximizing the benefits offered by ecological services in the Yanhe watershed.

Keywords Land use change · SWAT model · LCM · Water flow regulation · Erosion regulation · Mapping

Responsible editor: Marcus Schulz

Electronic supplementary material The online version of this article (https://doi.org/10.1007/s11356-017-0499-8) contains supplementary material, which is available to authorized users.

✉ Jing Li
lijing@snnu.edu.cn

[1] School of Geography and Tourism, Shaanxi Normal University, Xi'an, Shaanxi 710119, China

[2] National Demonstration Center for Experimental Geography Education, Shaanxi Normal University, Xi'an, Shaanxi 710119, China

[3] College of Geomatics, Xi'an University of Science and Technology, Xi'an, Shaanxi 710054, China

Introduction

The Yanhe river in China's loess plateau is well known for its relatively low water yield compared with its large sediment loads (Zhou and Li 2015). Human intervention through land use changes and soil and water conservation measures (Wang et al. 2015), combined with climate change (e.g., temperature and precipitation), has led to significant decreases in water production and sediment load. These changes directly affect the ecosystem services (ESs) that humans derive from the watershed ecosystem, and the evaluation of ecosystem services tends to act as a suitable method for evaluating and managing watershed ecosystems.

According to previous studies, climate change and land use/cover change are the main driving factors affecting

landscape patterns and ecosystem processes (Peng et al. 2017). Accordingly, exploring the relationship between them is of great significance, enabling a better understanding of regional and global environmental changes and helping advance research on ecosystem services. Climatic conditions, especially hydrothermal conditions, determine the type, structure, and function of ecosystems, and their impact on ecosystem services is gradually increasing (Li and Fang 2016). Climate change can have varying degrees of stress on ecosystems, while the provision of ecosystem services is also affected. For example, crop production, water supply, and wildlife biodiversity (Bellard et al. 2012) will be directly affected by climate change. Furthermore, ecosystem-regulating services, such as water regulation and sediment erosion regulation, are indirectly affected by climate change due to changes in surface vegetation (Hao et al. 2017; Luo et al. 2014). Land use is closely related to human activity, which affects ecosystem services by changing the types, patterns, and ecological processes of the underlying ecosystem. Initially, the ecosystem services and functions of different land use types are quite different and have a different impact on human well-being (Pullanikkatil et al. 2016; Quintas-Soriano et al. 2016). In addition, land use change can directly or indirectly affect ecosystem processes, leading to changes in biogeochemical cycles and the hydrological cycle. The changes in ecosystem state, structure, and function will influence the provision of ecosystem services (Wu et al. 2014; Zhao et al. 2015). Land use changes, such as deforestation, the increase and intensification of agricultural land use, and the expansion of urban lands in watersheds, are the primary driving forces affecting the water flow regulation services and the erosion regulation services (Jiao et al. 2017; Sun et al. 2014).

In recent years, many studies have been conducted that primarily focused on the application of a hydrological modeling approach to examine the hydrological impacts of land use change and/or climate variability (Fan and Shibata 2015; Pervez and Henebry 2015; Yesuf et al. 2015). The findings of these studies are helpful for understanding the causes of hydrological variations, as well as for developing adaptation measures. However, the effects may vary spatially due to their geographical differences, necessitating further investigation at a regional scale. Moreover, previous studies primarily focused on historical land use change and/or climate change and their impacts, ignoring the need for updating the climate and/or land use data to reflect current conditions (Lin et al. 2015; Zuo et al. 2016). Therefore, the results of these studies do not accurately represent the variation tendencies or spatial distribution patterns of future hydrological factors of the study area. Given the uncertainty of the future and the demands from administrations and policymakers, scenario simulation is an important tool for studying future ecosystem services. While an adequate amount of research on the potential impacts of climate change on water resources and water quality has been conducted, most of these studies did not integrate future land use configurations in their analyses; rather, they established climate change scenarios on the basis of general circulation model (GCM) projections (Panagopoulos et al. 2014; Pervez and Henebry 2015; Shrestha et al. 2017; Wilson and Weng 2011). As we know, the hypothetical climate scenarios that were established through the analysis of long-term climate observations may seem more reliable than GCM climate scenarios for a relatively small region with high spatial heterogeneity and complex terrain, as a result of the inherent coarse resolution of GCMs and their variable projections. There have been many studies that have investigated the uncertainty of GCMs, and these studies have found that these aforementioned issues are often the largest sources of uncertainty (Chen et al. 2011; Woldemeskel et al. 2012; Zhang et al. 2014b). To reduce the model uncertainties caused by errors in the input data, such as rainfall and temperature, climate projections in this study were produced using results from the statistical analysis of long-term climate observations.

Ecosystem mapping is a quantitative description of the spatial distribution of ecosystem services at a spatiotemporal scale that is determined through appropriate mapping evaluation methods that are based on specified decision requirements (Fu et al. 2013). The quantifiable information supporting these maps is an important contributions towards the application of the ecosystem service approach in science and in practice (Burkhard et al. 2012). The characteristics of the spatiotemporal distribution associated with the case study cannot be neglected in the quantification and mapping of the selected ecosystem-regulating services, especially for water-related ecosystem services, because hydrological processes act differently among climatic zones at the global scale (Zhang et al. 2015). The plateau continental monsoon climate in the selected study area exhibits a sharp seasonal contrast: hot summers and cold winters, with snowfall in winter. It is necessary to model and map seasonal differences in the selected ecosystem-regulating services for the study area. In addition to considering these often-neglected, spatiotemporal aspects in the quantification and mapping of ecosystem services, the objectives of this study were to develop a suitable indicator set, apply the identified set to address hydrological landscape processes, and map the selected ecosystem-regulating services in the Yanhe watershed.

In this study, we developed an ecological-hydrological model that conforms to the current conditions of the watershed and applied it to simulate and evaluate the ecosystem services in the Yanhe watershed. Additionally, through cartographic synthesis, a comprehensive feature map of the final ecosystem

services in the watershed is provided so participants can design optimized management approaches that consider ecosystem services.

Materials and methods

Study area

This study was conducted within the Yanhe watershed, which is part of the loess plateau (Fig. 1) and is located in northern Shaanxi province, China. The Yanhe river, a first-order tributary in the middle reaches of the Yellow river, starts in the Baiyu mountains in Jingbian county, Shaanxi province. It then flows through Zhidan county, Ansai, Yanan, and Yanchang county and drains into the Yellow river in Yanchang county. The basin covers an area of 7685 km^2 and lies between 36° 27′ and 37° 58′ N and between 108° 41′ and 110° 29′ W.

The watershed is in a warm temperate zone, with an average annual precipitation of approximately 520 mm that is concentrated in the summer. The altitude varies between 479 and 1787 m above sea level, and the average elevation is 1212 m above sea level. Floods usually accompany substantial watershed soil erosion in July and August. The average annual runoff and sediment loads are 2.94 × 108 m^3 and 0.882 × 108 t, respectively; nearly 80% of this is concentrated during the rainy season that occurs from June to September.

SWAT model description and setup

The soil and water assessment tool (SWAT) model is a river basin-scale model developed by the United States Department of Agriculture (USDA) Agricultural Research Service (ARS) to predict the effects of land management practices on water sediment and agricultural chemical yields (Abbaspour et al. 2015; Meaurio et al. 2015; Uniyal et al. 2015). In SWAT, a watershed is divided into multiple sub-basins, which are then further subdivided into a series of hydrologic response units (HRUs) based on their unique soil, land use, and slope characteristics (Her et al. 2015; Ning et al. 2015). The hydrologic cycle for each HRU is simulated based on the water balance, which includes precipitation, interception, evapotranspiration, surface runoff, and lateral return and groundwater flows. The surface runoff is estimated with a modified soil conservation services (SCSs) curve number equation in each HRU using daily precipitation data (Zuo et al. 2016). The sediment yield is calculated within each HRU based on the empirical modified universal soil loss equation (MUSLE) developed by Williams and Arnold (1997), which uses the amount of runoff to simulate erosion and sediment yields. The model is thoroughly described in the SWAT theoretical documentation (Neitsch et al. 2011).

The SWAT model requires numerous data inputs, including a digital elevation model (DEM), land use and soil maps, a time series of climate data, and information regarding land management (Table 1). In this study, we used the DEM to derive the stream network and to delineate sub-basins. To do so, we selected a threshold drainage area of 150 km^2. The entire process produced a total of 25 sub-basins. To define the HRUs, we derived a slope map from the DEM and divided it into five classes, introducing breaks at 5, 15, 25, and 45%. As suggested by (Qiu et al. 2012), we used thresholds of 5, 5, and 5% for land use, slope, and soil, respectively. This gave us a total of 240 HRUs. Daily meteorological data were then fed into the model. We used precipitation, wind speed, humidity, sunshine duration, and maximum and minimum temperature data from six stations (Fig. 1).

Model sensitivity, calibration validation, and uncertainty analyses

The SWAT model sensitivity, calibration, and validation, as well as uncertainty, analyses were conducted for the sub-basins using the sequential uncertainty fitting, ver. 2 (SUFI-2) global sensitivity analysis procedure embedded in the SWAT calibration uncertainty programs (SWAT-CUP) (Panagopoulos et al. 2015). In the SUFI-2 algorithm, uncertainty sources (such as rainfall data, soil data, land use data, observed data, and parameters) are calibrated to encompass most of the measured data within a 95% prediction uncertainty (95PPU). Two indices are used to quantify the strength of the calibration/uncertainty performance: the *P* factor (value closer to 1 indicates better simulation results), which is the percentage of the measured data bracketed by the 95PPU band, and the *R* factor, which is the ratio of the average width of the 95PPU band and the standard deviation of the measured data.

The SUFI-2 algorithm, when applied separately to runoff and sediment load, also provides the sensitivity of the 12 parameters governing runoff and of the 8 parameters governing sediment load. These parameters are known to influence the stream flow and sediment yield in similar catchments and are significant in representing the effectiveness of the SWAT model in the study area (Li and Zhou 2015; Yan et al. 2017; Zuo et al. 2016). The name of each parameter, the variation method, the uncertainty ranges, the optimal value, and their ranking based on *t* statistics are listed in Tables 2 and 3. Table 2 shows that the most sensitive parameters for runoff are the SCS runoff curve number (CN2), the soil evaporation compensation factor (ESCO), and the moist bulk density of the soil layer (SOL_BD). Sediment load simulations were conducted based on the hydrological simulations, which were calibrated for the study. Table 3 shows that the most sensitive parameters for sediment were the USLE equation

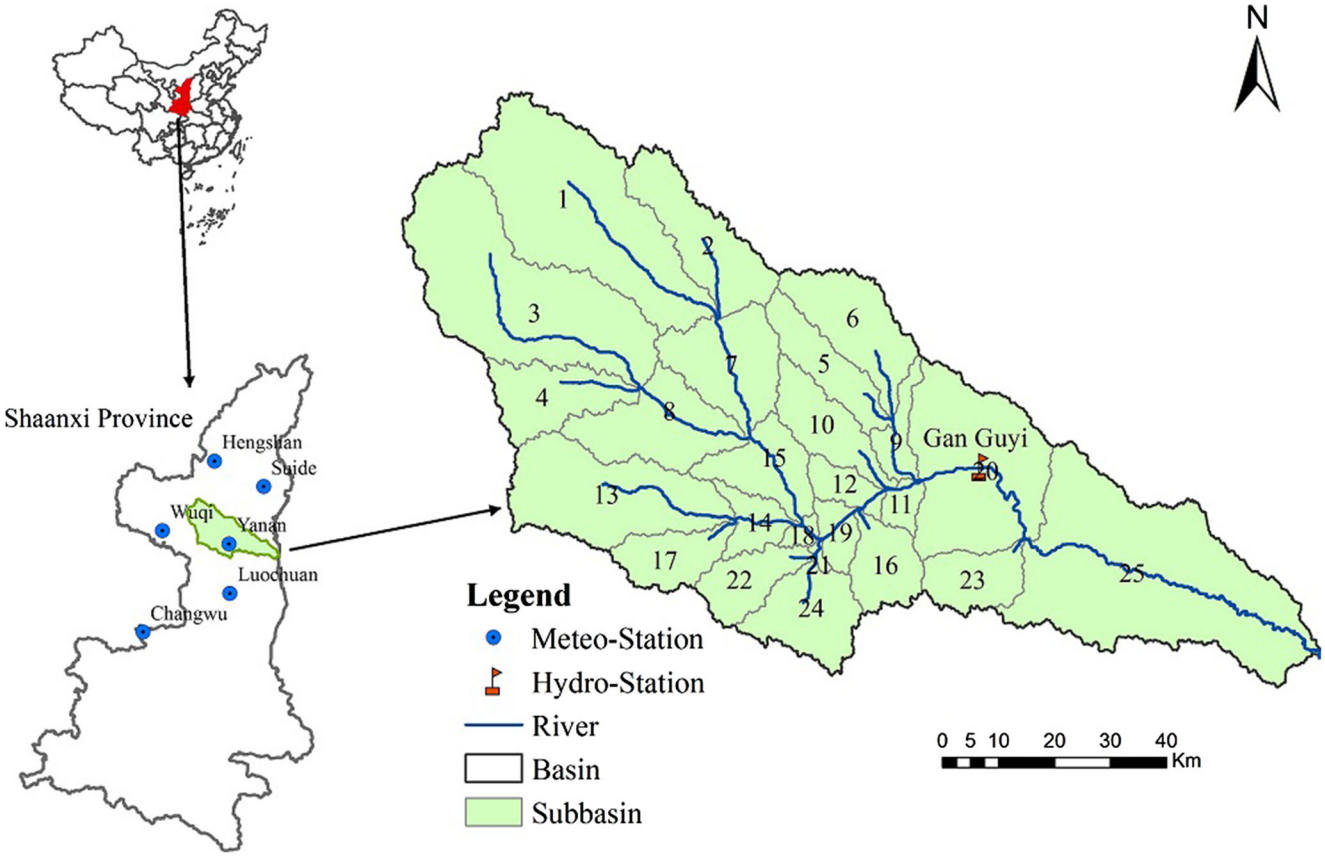

Fig. 1 Location of the study area and gauging stations

support practice factor (USLE_P) and the average slope steepness (HRU_SLP).

We then considered the most sensitive parameters, as suggested by the sensitivity analysis, for model calibration and validation. We chose the Nash-Sutcliffe efficiency (NSE) as an objective function. However, the model performance was also evaluated according to the coefficient of determination (R^2) as well as the SUFI-2 *P* and *R* uncertainty factors. Model performance is judged as "satisfactory" if $R^2 > 0.5$ and NSE > 0.5 for the runoff and sediment yield monthly time-step evaluation (Meaurio et al. 2015). The results of the simulated model for runoff and sediment yield are suitably consistent in terms of both time and volume with the corresponding observed values. The model's calibration period for simulating runoff was 1991–1998; the period between 1999 and 2006 was the validation period (runoff: *P* factor = 0.6, *R* factor = 1.03, R^2 = 0.75, NSE = 0.71 for 1991–1998 calibration; *P* factor = 0.56, *R* factor = 1.24, R^2 = 0.68, NSE = 0.64 for 1999–2006 validation). The model's calibration period for simulating sediment load was 1997–2002; the period 2003–2008 was the validation period

Table 1 Data inputs used and their sources

Input data	Resolution	Source
DEM	30 m	Computer Network Information Center, Chinese Academy of Sciences (http://www.gscloud.cn/)
Land use map	30 m	Data Center for Resources and Environmental Sciences, Chinese Academy of Sciences (http://www.resdc.cn)
Soil-type map	1000 m	Institute of Soil Science in Nanjing, Chinese Academy of Sciences
Meteorological data	Daily	Meteorological Administration of Yanan City
Hydrological data	Daily	Yellow River Conservancy Commission

Table 2 Parameter sensitivity analysis results for runoff in the Yanhe watershed

Change type	Parameter	Description	Global sensitivity			Optimal value
			t value	*p* value	Rank	
R	CN2.mgt	SCS runoff curve number (–)	− 17.258	0.000	1	↑10%
V	ESCO.hru	Soil evaporation compensation factor (–)	− 9.398	0.000	2	0.63
R	SOL_BD.sol	Moist bulk density (g/cm^3)	− 8.780	0.000	3	↓14%
V	CH_K2.rte	Effective hydraulic conductivity in the main channel alluvium (mm/h)	− 8.775	0.000	4	10.75
V	SFTMP.bsn	Snowfall temperature (°C)	2.239	0.0253	5	−4.94
V	CH_N2.rte	Manning's roughness coefficient for main channel flow (-)	− 2.153	0.5373	6	0.145
V	GW_REVAP.gw	Groundwater revap. coefficient) (–)	1.408	0.159	7	0.12
V	ALPHA_BF.gw	Base flow alpha constant (days)	1.332	0.257	8	0.49
R	SOL_K.sol	Saturated hydraulic conductivity (mm/h)	− 0.606	0.544	9	↓17%
V	EPCO.hru	Plant uptake compensation factor (–)	− 0.598	0.550	10	0.48
R	SOL_AWC. sol	Available soil water capacity (mm H_2O/mm soil)	− 0.456	0.648	11	↓11%
V	GW_DELAY.gw	Groundwater delay time (days)	0.138	0.889	12	168

R parameter value is multiplied by (1 + a given value), *V* parameter value is replaced by given value

(sediment yield: *P* factor = 0.51, *R* factor = 1.38, R^2 = 0.67, NSE = 0.61 for 1997–2002 calibration; *P* factor = 0.35, *R* factor = 0.83, R^2 = 0.56 NSE = 0.52 for 2003–2008 validation). Model calibration and validation details are provided in Figs. 2 and 3.

Future climate data and model simulations

The NCC/GU-WG 2.0 is a climate forecast model based on a statistical technique that enables the simulation of various important climatic factors (including precipitation, the highest and lowest temperatures, and sunshine time) and was developed by China's meteorological administration climate center. It has been commonly applied to large areas in China (Liao et al. 2013). The NCC/GU-WG 2.0 produces dry and wet daily data series using the first-order Markov Chain method, simulates wet-day rainfall using the two-parameter gamma distribution model, and estimates daily non-precipitation variables based on a precipitation simulation process (Liao et al. 2009).

Table 3 Parameter sensitivity analysis results for sediment in the Yanhe watershed

Change type	Parameter	Description	Global sensitivity			Optimal value
			t value	*p* value	Rank	
V	USLE_P.mgt	USLE equation support practice factor	− 6.582	0.000	1	0.27
R	HRU_SLP.hru	Average slope steepness	− 6.512	0.000	2	↓11%
V	SPCON.bsn	Linear parameter for calculating the maximum amount of sediment that can be re-entrained during channel sediment routing	− 5.824	0.000	3	0.009
R	USLE_K.sol	USLE equation soil erodibility factor	− 2.745	0.006	4	↑8%
V	CH_COV2.rte	Channel bed erodibility factor	− 2.725	0.023	5	0.31
R	SLSUBBSN.hru	Average slope length (m)	1.443	0.149	6	↓5%
V	CH_ COV1.rte	Channel bank erodibility factor	− 1.312	0.188	7	0.52
V	SPEXP.bsn	Exponent parameter for calculating sediment re-entrained in channel sediment routing	− 0.885	0.376	8	1.033

R parameter value is multiplied by (1 + a given value), *V* parameter value is replaced by given value

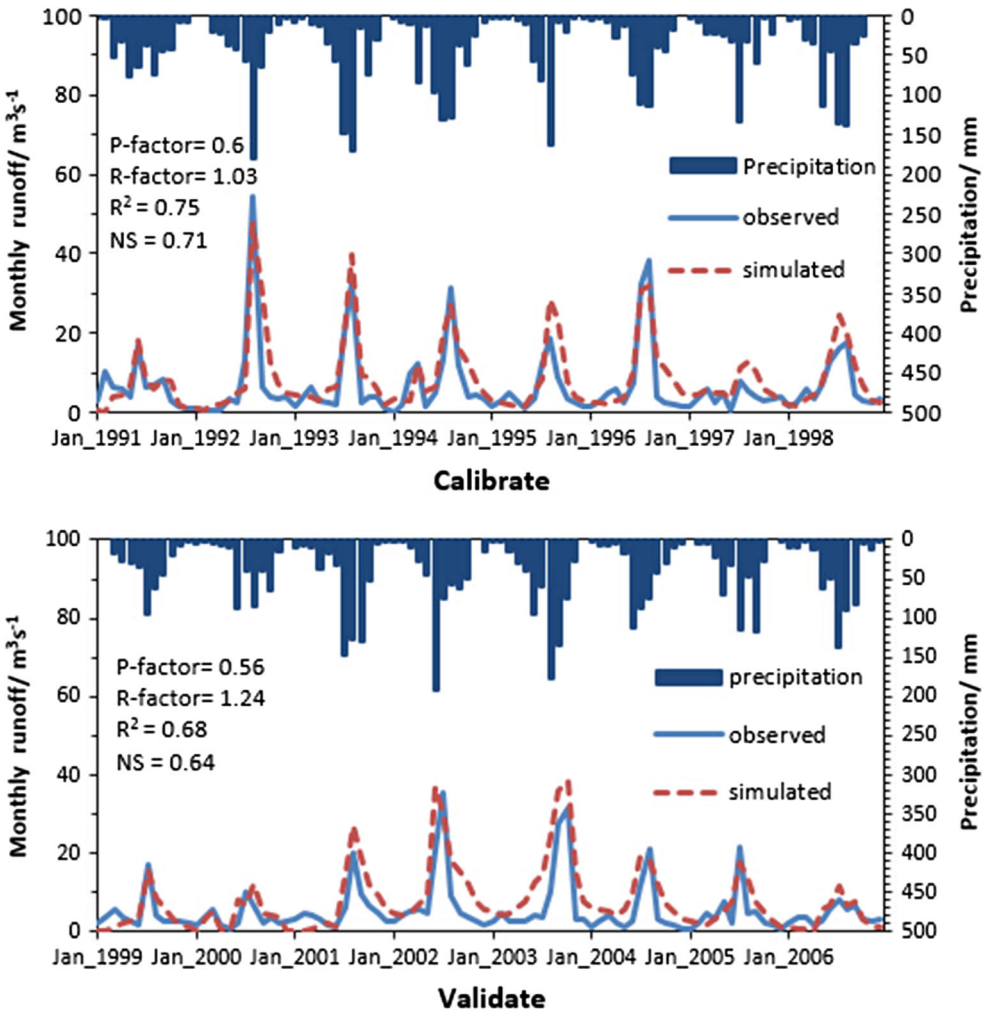

Fig. 2 Monthly runoff yield during the calibration period (1991–1998) and validation period (1999–2006)

In this study, we simulated daily climate datasets (including maximum temperature, minimum temperature, and precipitation) for six weather stations for the period 2021–2060. Due to the strong seasonal variation, it is necessary to model and map seasonal differences in the selected ecosystem-regulating services for the study area. When assessing the regulation services under future climate conditions, four different time segments were selected to address strong seasonality:

1) Monthly average values for 2050;
2) March, which is the period of snowmelt;
3) July/August, when the highest precipitation occurs during the rainy season; and
4) November, which is the month with the most snowfall.

Future land use change scenarios

Land change modeler (LCM) for ecological sustainability is an integrated software module in IDRISI that allows for the prediction and analysis of land cover change and assesses habitat and biodiversity impacts (Yang et al. 2014). In this paper, we chose several driver variables, including DEM, slope, proximity to roads, proximity to rivers, and proximity to the city center, to analyze the changes in historic land cover. Subsequently, empirical land cover change-modeling methods were used to relate historic land cover changes to the driver variables; thus, a set of rules could be extracted and extrapolated into the future.

We also used the LCM to identify and incorporate planning intervention maps that may alter the course of development. Planning interventions include constraints and incentives, such as the development of roads and policy initiatives, in addition to the year when such changes will become effective (Lin et al. 2014). We set the area that needs to be preferentially converted into other land use types to 1, the region where conversion is limited to − 1, and the region where land use is basically unchanged to 0. By doing so, we predicted the possible future changes and use of the land cover under different policy planning scenarios.

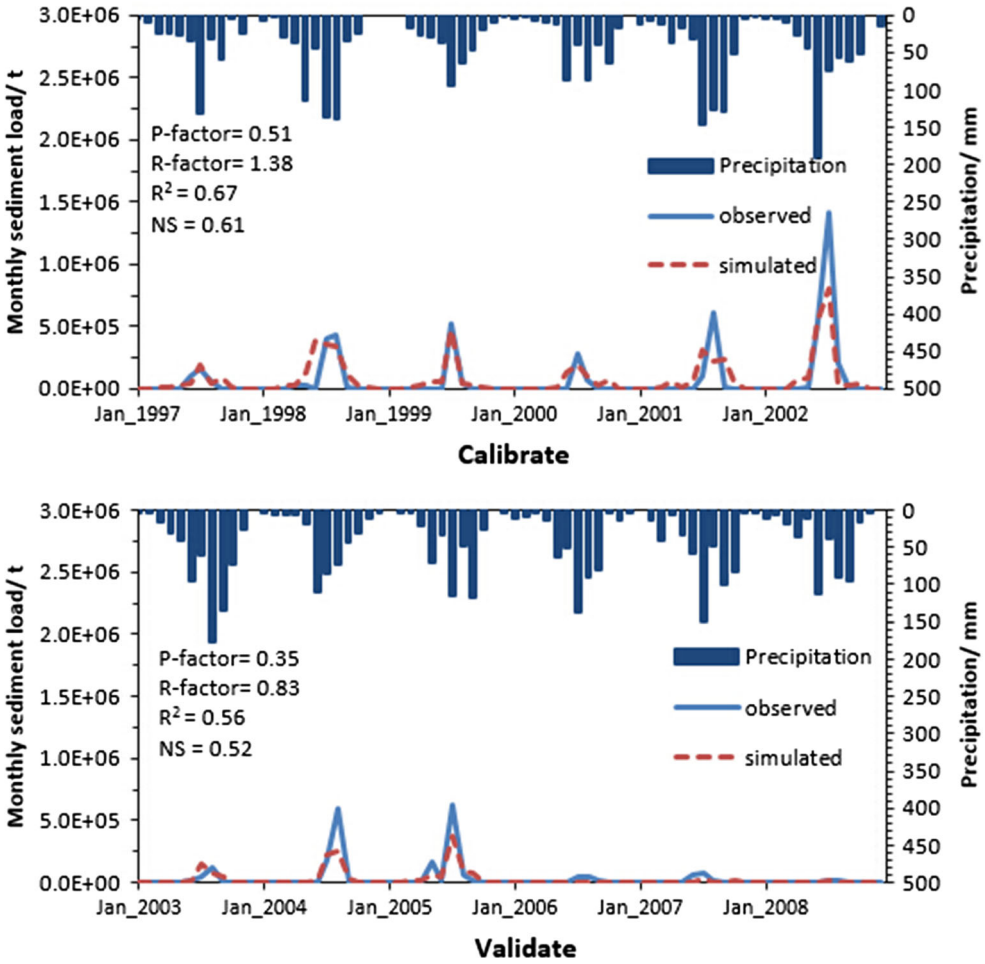

Fig. 3 Monthly sediment load during the calibration period (1997–2002) and validation period (2003–2008)

Policy planning scenario 1 refers to the progress of urbanization with certain constraints, in which the main policy is returning farmland to forest and grassland; this scenario includes the typical characteristics of low urbanization and abundant hillsides that facilitate afforestation. We set the mountainous area with a slope greater than 15° as a protected forestland, and we increased the probability of conversion to other land use types to forestland and grassland. In addition, we strengthened family planning in areas with a slope under 15° to control for population growth and to limited the conversion of other land use types to urban land and agricultural land.

Policy planning scenario 2 promotes socioeconomic development to ensure the satisfaction of human demand. It also drives the construction of an ecologically minded civilization that is supported by an ecological protection policy, achieves sustainable development, and formulates appropriate land use policies. In scenario 2, the rough terrain (slope > 25°), which is not suitable for the development of industry, agriculture, and population growth, is transformed to forestland and grassland, with an expansion buffer area, where the probability of conversion to industrial land, urban development, and agricultural land is low. Agricultural land with food crops, such as wheat and corn, is limited to gentle slopes of less than 15°, while cultivated land (15° < slope < 25°) is preferentially converted into fruit tree plantations.

Policy planning scenario 3 drives an unprecedented process of urbanization and exploitation of natural resources based on the current trend of economic development. With the growth of the economy, an increase in population, and the processes of industrialization and urbanization, human demand for land resources is increasing. A large percentage of the population migrates from rural to urban areas and engages in non-agricultural work. The surrounding urban areas located within 1 km of the flat regions (slope < 10°) are set as an urban expansion buffer, with a large probability of converting other types of land into urban land.

The approach applied in this paper comprises three steps. First, we used land use maps from 1990 to 2000 to simulate land use maps for 2010 with the LCM (Fig. 4). Second, the CROSSTAB model in IDRISI was used to compare the simulation results and the actual 2010 land use map, cell by cell, to validate the reliability of the model developed in this

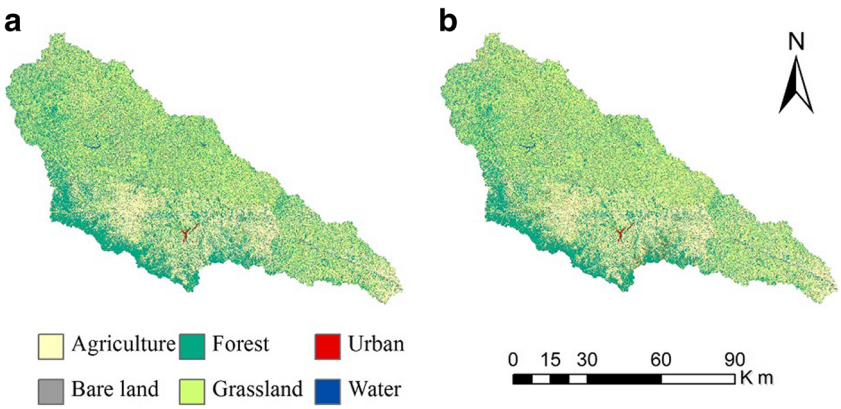

Fig. 4 Land use maps. **a** Actual land use in 2010 and **b** simulated land use in 2010

paper. The results of the cross-tabulation analysis are shown in Table 4. The simulated area, actual area, error rate (rate of error area), and kappa index of agreement (KIA, using the actual land use map as the reference image) are listed by land use categories. In terms of quantitative accuracy, the absolute value of the error rate for all classes is less than 0.2. In terms of spatial accuracy, the KIA for all classes is greater than 0.75, which is acceptable. The agreement between the actual area and simulated area is judged as "good" if KIA > 0.6 (Pérez-Vega et al. 2012; Pontius and Schneider 2001). This indicates that the LCM can simulate the study area's future land use patterns accurately and objectively and can be used for further research. Last, based on the validated LCM, the actual land use maps from 2000 and 2010 were used to generate the land use maps for 2050 under different planning and policy scenarios, and the changes were analyzed.

Procedure for data analyses using the "matrix approach"

We used the outputs of the SWAT model, which included water flow and sediment yield, to quantify and map the water-related regulation services under all three scenarios. The procedure of our SWAT model output data analysis is based on three steps:

1. Water yield and sediment yield were calculated to analyze the changes in all three scenarios.
2. Model output values were transformed into a relative scale from 1 to 5 (low to very high supplies of ecosystem services) following the method proposed by Burkhard et al. (2014), Burkhard et al. 2012).
3. Two water-related regulation services were mapped for spatial visualization.

Calculation of indicators for two selected regulation services under all three scenarios

The spatial distribution of the SWAT model outputs at the sub-basin level was visualized to locate the exact spatial distributions and to link the model outputs to the generated spatial map. The regulation services "water flow regulation" and "erosion regulation" can be best quantified using indicators available for the entire sub-basin. In the first step, the water yield (WYLD) and the sediment yield (SYLD) were selected as the indicators to quantify the water-related ecosystem services for all three scenarios. Then, the monthly averages of WYLD and SYLD over three selected periods in 2050 were calculated for each sub-basin (Table 5).

Table 4 Comparison of the accuracy for simulated areas and actual areas

	Actual 2010		Simulated 2010		Error rate	KIA
	Area (km^2)	Percent (%)	Area (km^2)	Percent (%)		
Agriculture	1914.22	24.91	1988.42	25.87	0.039	0.764
Forest	2441.66	31.77	2333.66	30.36	− 0.044	0.874
Grassland	2689.62	34.99	2716.24	35.34	0.01	0.897
Water	48.81	0.64	48.77	0.63	− 0.001	0.890
Urban	307.77	4	344.53	4.49	0.119	0.884
Bare land	283.83	3.69	254.29	3.31	− 0.104	0.763

Table 5 Model outputs of all sub-basins (n = 25) for three scenarios, each with four periods and two indicators for regulation services

Regulation service	Indicator	Scenario 1				Scenario 2				Scenario 3			
		Mean	Mar	Jul/Aug	Nov	Mean	Mar	Jul/Aug	Nov	Mean	Mar	Jul/Aug	Nov
Water flow regulation	WYLD (mm)	1.63	1.48	4.64	1.25	2.01	1.93	5.84	1.62	2.46	2.45	7.2	2.05
Erosion regulation	SYLD (t/ha)	0.027	0.013	0.162	0.01	0.036	0.016	0.22	0.015	0.04	0.02	0.27	0.02

WYLD water yield (mm), *SYLD* sediment yield (t/ha), *Mean* monthly average, *Jul/Aug* the average of July and August

Transformation of the model output values into a relative scale

In the second step, the indicators and their simulated values for the regulation services were assessed on a relative scale from 1 (low regulation) to 5 (high regulation). This methodology follows the "matrix approach" (Jacobs et al. 2015); however, the scale was not extended to the 0 class because there were no values defined as "no regulation." We specified the ranges through the minimum and maximum values of the indicators for all scenarios (based on Table 5). The range of indicators was divided into five equal classes and assigned to the 1–5 scale using "appropriate class breaks" (Table 6). Schmalz et al. (2016)) indicate that "appropriate class breaks" are important for the application of this relative scale when discussing the results with stakeholders. Table 6 clearly shows the ranges of WYLD and SYLD and their corresponding levels of ecological regulation services.

Mapping the ecosystem services for spatial visualization

Ecosystem service mapping, which is attracting growing interest for presenting visualizing assessment results and the spatial distributions of ecosystem services, is a powerful tool that helps policymakers locate spatial mismatches among ecosystem services and formulate related management actions (Karabulut et al. 2016).

The maps of the water-related ecosystem services were generated by assigning the calculated values of the water yield and sediment yield in a geographic information system (ArcGIS). The explicit spatial distribution of the water flow regulation services and the erosion regulation services, along with the temporal scale for all three scenarios, is shown in the maps based on the sub-basin scale.

Results

Analysis of predicted land use change between 2010 and 2050

In this paper, according to the actual situation, the trend of land use change, and the usefulness of the available data for the Yanhe watershed, we chose five driving variables, including three spatial distance factors (rivers, roads, and cities) and two natural factors (DEM and slope); set the constrained and incentive mechanisms linked to the three policy scenarios; and generated three kinds of land use maps for 2050 (Fig. 5).

The 2010 map and the three 2050 maps of the extents of the land cover classes were compared based on percent composition of the entire watershed (Fig. 6). Of all three 2050 land uses, forest and grassland were the two most common land use types in the Yanhe watershed, composing approximately 70% of the entire watershed. This distribution is closely related to policies that drive the return of farmland to forest and grassland, and long-term and large-scale afforestation activities greatly improve the watershed's vegetation coverage rate. In 2050_Scenario1, the forest increased by 5% (or 379.4 km^2), the agricultural land decreased by 5.1% (or 395.6 km^2), and the other land use types only slightly changed compared with those in 2010.

In 2050_Scenario2, the largest increase occurred in urban land, which more than doubled compared with that in 2010, accounting for 8.06% (or 619.72 km^2) of the entire watershed; this was followed by grassland, which accounted for 38.21% (or 2937.01 km^2) of the entire watershed. The growth of urban spaces was primarily a result of the conversion of agricultural lands with a low slope. The agricultural land decreased by 6.2% (or 472.8 km^2) compared to that in 2010. In

Table 6 Relation valuation scale for the quantification of water flow regulation and erosion regulation based on the SWAT model results

Class	Water flow regulation	Erosion regulation	WYLD (mm)	SYLD (t/ha)
1	Very low water flow regulation	Very low erosion regulation	0–2.5	0.7–1
2	Low water flow regulation	Low erosion regulation	2.5–5	0.5–0.7
3	Medium water flow regulation	Medium erosion regulation	5–7.5	0.3–0.5
4	High water flow regulation	High erosion regulation	7.5–10	0.1–0.3
5	Very high water flow regulation	Very high erosion regulation	> 10	< 0.1

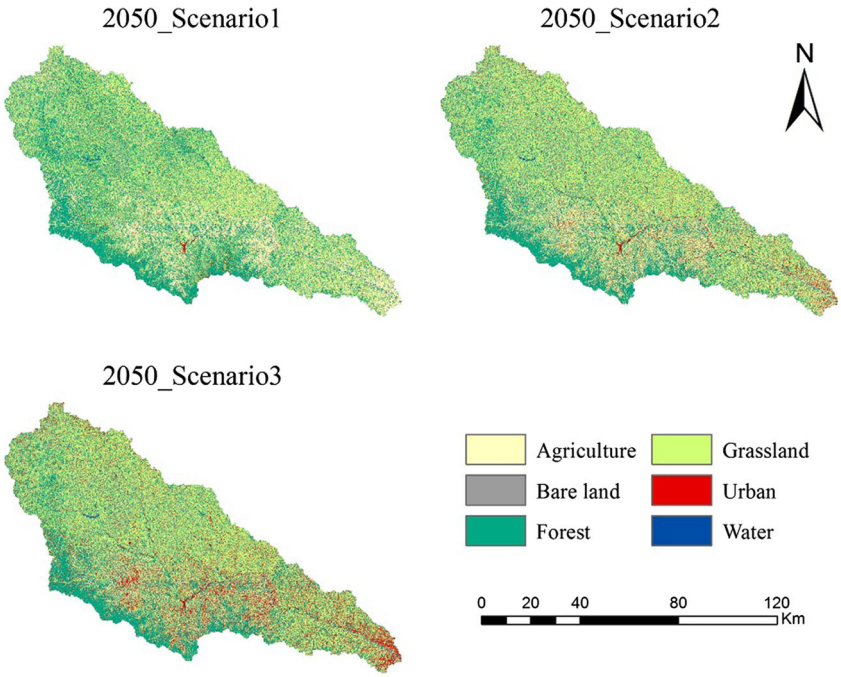

Fig. 5 Three simulated land use maps for 2050, based on different scenarios

2050_Scenario2, along with the accelerated process of urbanization and the increasing demand for urban areas, a large amount of agricultural land was lost in many low-lying regions along the middle and lower reaches of the Yanhe river. Agricultural land was sharply reduced from 24.91% (or 1914.22 km^2) to 12.72% (or 980.88 km^2). However, urban land increased dramatically, from 4% (or 283.83 km^2) to 14.36% (or 1103.71 km^2), compared to that in 2010. This is strongly related to human activities, such as "cut the mountain and fill the gully," to expand city construction.

The effects of land use changes on ecosystem services

As Table 5 shows, the values for water yield and sediment erosion show very significant differences among the different scenarios. The average monthly sediment erosion is low, at 0.027 t/ha in scenario 1, which is less than the values of 0.036 t/ha in scenario 2 and 0.04 t/ha in scenario 3. The average monthly water yield for the different scenarios also shows the same pattern. The highest simulated water yield and sediment erosion occurred in scenario 3, followed by scenario 2 and scenario 1. The differences among them are the most obvious in July/August. To further analyze the impact of land use change on water yield and sediment yield, we selected the most obvious changes in four land use types, water yield, and sediment yield in July/August among the different land use scenarios (details in Table 7). For example, we conducted an analysis between scenario 3 and scenario 1. The water yield and sediment yield in July/August increased by 2.56 mm and 0.108 t/ha, accounting for 55.17 and 66.67%, respectively, of the simulated results in scenario 1. The amounts of agricultural and forestland are 980.88 and 2392.78 km^2, respectively, in scenario 3, values which are far lower than their corresponding values of 1518.59 and 2821.01 km^2 in scenario 1; the percentage decreased by 35.41 and 15.18%, respectively. In contrast, the amount of urban land in scenario 3 is 1103.71 km^2, which is far higher than the value of 344.95 km^2 in scenario 1, and the percentage increased by 219.96%. The obvious decreases in farmland and forestland and the increase in urban land are caused by deforestation for

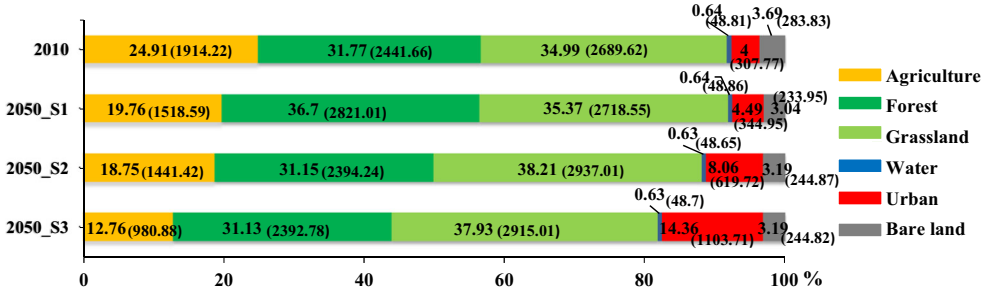

Fig. 6 Comparison of the 2010 and 2050_ Scenario1, 2050_ Scenario2, and 2050_Scenario3 extents of land use classes based on percent composition of the Yanhe watershed (study area = 7762.5 km^2). Areas are given in square kilometers for each LULC class

Table 7 The changes in primary land use and two indicators for ecosystem-regulating services among different land use scenarios

Variable	S1	S2	S3	(S2 − S1)/S1 (%)	(S3 − S2)/S2 (%)	(S3 − S1)/S1 (%)
Agriculture	1518.59	1441.42	980.88	− 5.08	− 31.95	− 35.41
Forest	2821.01	2394.24	2392.78	− 15.13	− 0.06	− 15.18
Grassland	2718.55	2937.01	2915.01	8.04	− 0.75	7.23
Urban	344.95	619.72	1103.71	79.66	78.1	219.96
WYLD	4.64	5.84	7.2	25.86	23.29	55.17
SYLD	0.162	0.22	0.27	35.8	22.73	66.67

Agriculture, forest, grassland, urban are four land use types (km^2)

S1 scenario 1, *S2* scenario 2, *S3* scenario 3, *WYLD* the average water yield of July and August (mm), *SYLD* the average sediment yield of July and August (t/ha)

farmland reclamation and urbanization and are important factors affecting the reduction in water yield and the increase in sediment yield in this watershed. Transpiration from vegetation is responsible for directly returning more than half of the water that falls on the land back to the atmosphere. Although accelerating the large-scale afforestation efforts lowers sediment erosion, our research finds that doing so may also decrease the levels of available water resources.

The simulated model output values of indicators for the sub-basins and corresponding ES values

First, we analyzed the simulated SWAT model output variables for the sub-basins (Table 5). The water yield showed the highest values, which were up to 7.2 mm in July/August in scenario 3, and the lowest values occurred in November, i.e., 1.25 mm in scenario 1. The highest values are approximately three times larger than the lowest values. For all three scenarios, the monthly mean water yield values were roughly equal to the values in March. The maximum appeared in July/August, and the lowest appeared in November. This pattern corresponds to the climate characteristics, which means that precipitation shows great variability and is concentrated in the summer due to rainstorms in the study area.

The simulated sediment yield was the highest in scenario 3 and the lowest in scenario 1. The only exception was that the sediment yield in November in scenario 3 was slightly lower than that in scenario 2. In all three scenarios, the sediment yield showed the highest values (especially in scenario 3, up to 0.27 t/ha) in July/August, and the lowest values were simulated in November and March. It was obvious that the watershed sediment erosion was mainly triggered by rainstorms in the summer.

Second, the SWAT model outputs regarding indicators were transformed to a relative scale for the sub-basins (Table 8). When analyzing the water regulation, all values for the four periods and the three scenarios were greater than 1.00. In general, scenario 3 had the highest water production capacity. The monthly average of 1.36 was obtained because the July/August value of 3.24 was the highest, and the values in March and November were higher than those during the same periods in the other two scenarios. Scenario 1 had the lowest water production capacity and a monthly value of 1.08; the highest value of 2.24 was obtained in July/August, and the lowest value of 1.04 was obtained in November.

When analyzing the erosion regulation, scenario 1 had a maximum monthly average value of 4.92, followed by scenario 2 with a monthly average value of 4.8 and Scenario 3 with a monthly average value of 4.76. For all three scenarios, the values were greater than 4.8 in March and November and much higher in July/August. This indicates that erosion regulation ability in March and November is very high due to low erosion rates.

Spatial patterns of water flow and erosion regulation services

Finally, the spatial patterns within the watershed were analyzed. Concerning the water flow regulation (Fig. 7), the maps showed high seasonal differences, with the highest deviations in July/August under all three scenarios. The maps also showed the uneven spatial distribution of water flow regulation. Higher water flow regulation was calculated in the downstream areas of the Yanhe river due to high water yield.

By analyzing the erosion regulation, we can also conclude that significant seasonal differences occurred in all three scenarios (Fig. 8). For all three scenarios, high or very high regulation was calculated for all sub-basins in November. It is noteworthy that very high regulation occurred across the entire watershed, except in sub-basin 3 in March. The maps obviously depict an uneven spatial distribution of erosion regulation, especially in July/August. Low and very low regulations were calculated in the upper reaches of the Yanhe river due to high erosion rates.

Table 8 Mean values (a relative scale 1–5) of all sub-basins (n = 25) for calculated ecosystem services for the three scenarios, four periods, and two indicators of both regulation services

Regulation service	Indicator	Scenario 1				Scenario 2				Scenario 3			
		Mean	Mar	Jul/Aug	Nov	Mean	Mar	Jul/Aug	Nov	Mean	Mar	Jul/Aug	Nov
Water flow regulation	WYLD	1.08	1.12	2.24	1.04	1.12	1.12	2.92	1.04	1.36	1.4	3.24	1.12
Erosion regulation	SYLD	4.92	4.84	4.52	5	4.8	4.84	4.32	5	4.76	4.84	4.2	4.96

WYLD water yield, *SYLD* sediment yield, *Mean* monthly mean, *Jul/Aug* the average of July and August

Discussion

Both water yield and sediment yield were directly affected by land use/land cover changes and their management. The related impacts on human well-being act at different spatial and temporal scales, and these differences in impacts need to be understood when new management strategies are defined. The simulation and assessment of water and sediment yields under future climate and land use changes, which can be used to conduct optimized management and risk aversion of ecosystem services, are of great significance for the sustainable development of the human environmental system. The importance of maps for spatial planning and their usefulness in the stakeholder process during decision-making are clear. Furthermore, the effects of land use change on ecological services are worthy of discussion. In addition, the applied model is subject to both limitations and uncertainties, which need to be considered in decision-making and land use planning.

SWAT model uncertainty

The SWAT model has been widely applied to address a wide range of issues related to hydrological processes, ranging from catchment to continental scales. Furthermore, the SWAT model has gained international recognition. However, the SWAT model has a complex structure, requiring various parameters and data inputs that may be unavailable in specific forms

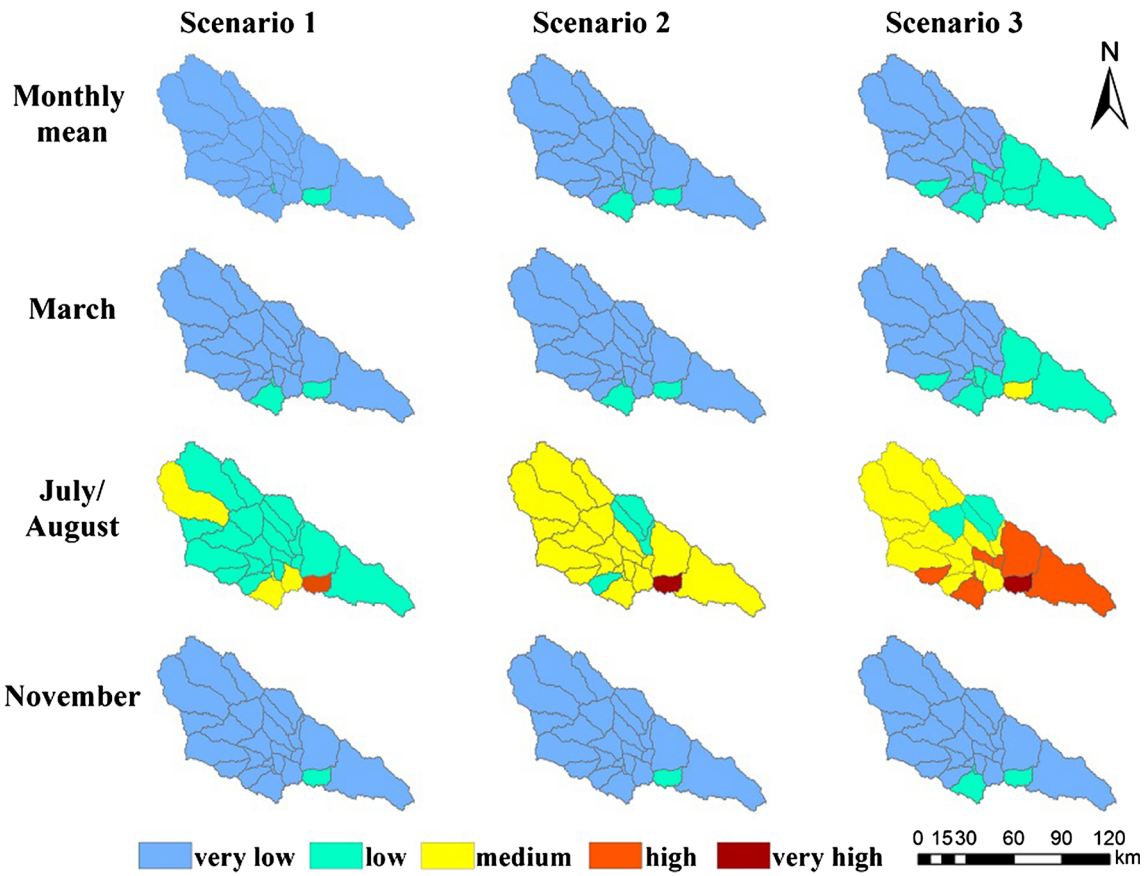

Fig. 7 Water flow regulation in the three scenarios, shown as monthly mean value and as values for March, July/August, and November (of 2050)

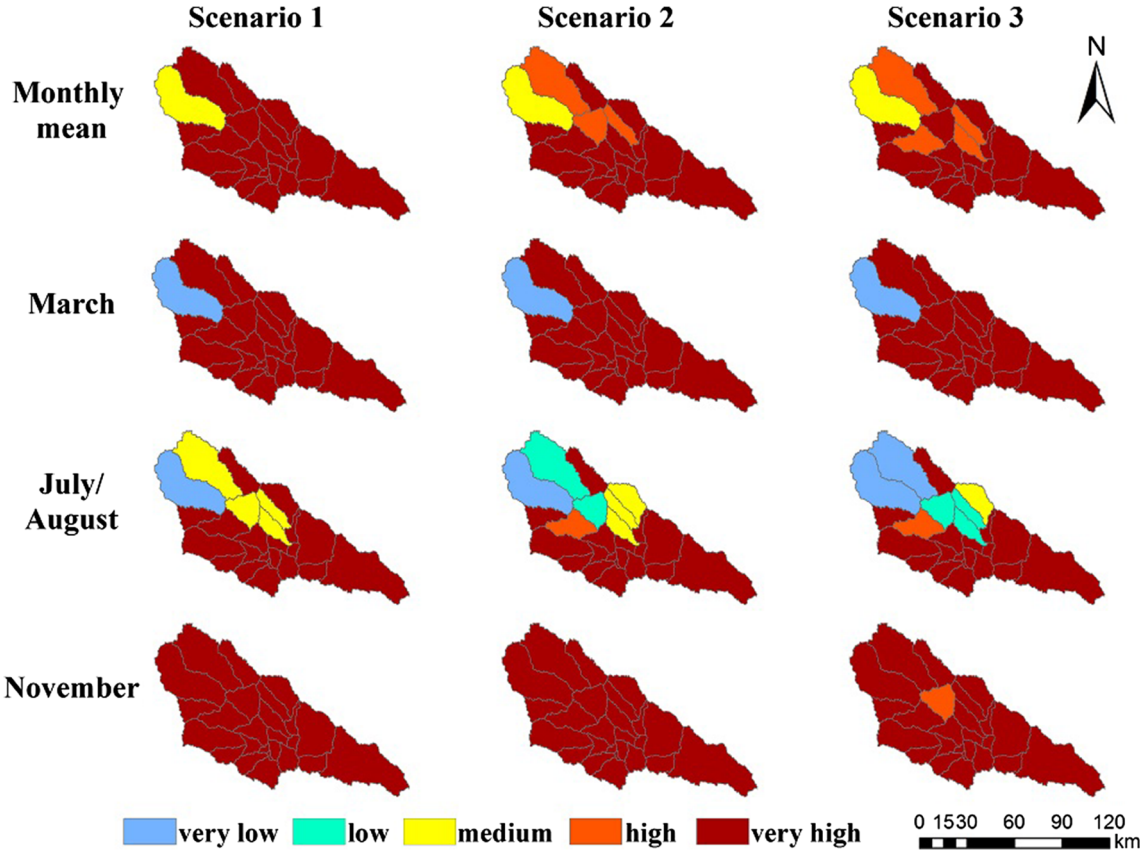

Fig. 8 Erosion regulation in the three scenarios, shown as monthly mean value and as values for March, July/August, November (of 2050)

(Ning et al. 2015; Vigerstol and Aukema 2011). In general, the simulations for different periods will have different input data (soil, land use, slope, meteorological data, etc.), which will lead to changes in the sensitivity and value ranges of the parameters (Abbaspour et al. 2015). For example, because DEM is one of the most important inputs for SWAT, it constitutes one of the main sources of uncertainty. Many studies have indicated that runoff, sediment yield, total nitrogen, and total phosphorous were essentially affected by the DEM, in addition to sources and resampling techniques (Tan et al. 2015; Xu et al. 2016; Zhang et al. 2014a). Moreover, rainfall input uncertainties are widely identified as being key factors in hydrological models; inaccuracies in the rainfall amounts directly affect the model simulations (Leta et al. 2015). Strauch et al. (2012)) believe that the use of point rainfall data to assess the rainfall over a basin is highly uncertain due to measurement errors and temporal and spatial variabilities.

Although the findings of previous studies are helpful for understanding the uncertainty of the SWAT model, relative studies aiming to assess and quantify the uncertainty in the Yanhe watershed need substantial additional work. As we know, the landscape patterns and ecological processes of different regions have intense spatial heterogeneity, and the climate, vegetation, soil, and topography all have significant diversities, necessitating further investigation at regional scales. In addition, the influence of water conservation projects, such as reservoirs and dams, on the yield and spatial distribution of the water resources has also been ignored. All of these considerations were excluded in this study but urgently need to be implemented in future work.

Analyzing LCM uncertainty and land use policy scenarios

In this paper, the LCM model was used to simulate land use changes in 2010, and this model has high simulation accuracy. We forecasted the spatial structure of land use in 2050 under different land use policy conditions. Data are the basis of building a model; therefore, the accuracy of the model is dependent on having a relatively complete set of accurate input data (Pérez-Vega et al. 2012; van Vliet et al. 2016). However, there are various limitations in terms of reality. The collected data resolution is not very high, affecting the classification accuracy of the remote sensing image. How to build a reasonable potential transformation model is of critical importance. In this paper, we selected the space distance factor and the natural factor as the driving variables to analyze the transformation potential among the various land use types, and we ignored the socioeconomic factors. Next, we need to

select more convincing driving variables to forecast future land use changes and spatial distribution.

Future land use changes are affected by many factors; it is a very complex and diversified development process (Yang et al. 2014). To build more reliable land use maps for 2050, the different land use policies were set for the intervening factors to constrain (or encourage) the development of land. In this study, the different land use scenarios have different regulation capabilities for the different indicators. Scenario 1 has the highest erosion regulation services and vegetation coverage and a good ecological environment, but it constrains economic growth. In scenario 3, due to the high degree of urbanization, the excessive use of natural resources leads to severe soil erosion and fragile ecological environments. Policymakers need to develop land use plans to manage these fragile ecosystems.

Ecosystem service quantification and visualization

The applied "matrix approach" method (Jacobs et al. 2015) has the ability to quantify different indicators and units in an integrative relative scale. However, several difficulties appear when transforming the simulated outputs into the relative scale. The class number differs according to the class width and the range of the maximum and minimum values. This is especially difficult when multiple values show extreme trends in one direction. This means that the scale is not showing the range of differences within the lower values in sufficient detail (Schmalz et al. 2016). Here, the water yield and sediment yield are so high during July/August that all values in the other seasons fall within a single class. Differences that occur during periods with low water and sediment yields are not properly represented. In addition, Burkhard et al. (2014)) also suggested using "appropriate class breaks," which are important for the application of this relative scale and in discussing the results with stakeholders. Therefore, the classes of the 1–5 scale were subdivided into categories with different widths, rather than equal intervals, in this research (Table 6).

Additionally, mapping is a powerful tool for displaying the water provisioning and regulatory services delivered by ecosystems (Rasul 2016). In our study, the quantifiable information for all three scenarios and time periods was presented with these maps. This offers the opportunity for stakeholders and decision makers to assess the future ecosystem services for the watershed. Watershed management and land use development policies are created and applied using common guidelines based on these simplified maps. For example, the class sizes are so large that for the monthly average water flow regulation, many calculated values fall within class 1 and represent very low water provisioning by the ecosystem. However, for July/August in scenario 3, most values fall in classes 3–5, implying that too much water exists on the landscape. Therefore, it is necessary to store the water resources to solve the problem of seasonally uneven distributions.

Spatial distribution

Due to the 1–5 scale, only a few spatial patterns are represented on the maps; however, high spatial resolution at the sub-basin scale can be recognized within these patterns, e.g., the distribution of water flow regulation in scenario 3 for July/August (Fig. 7). If we compare the water flow regulation patterns with the land cover/use map, we see high water flow regulation in residential areas and wet grasslands in the downstream region of the Yanhe river; most areas with other land cover/uses can be assigned to low or intermediate regulation. Spatial patterns of water flow regulation were also mapped for the same period (July/August) for scenario 1 and scenario 2 but obviously decrease across the entire watershed compared to those in scenario 3. A closer look at the monthly mean for all three scenarios shows that the central and downstream regions are characterized by low regulation, while the forested areas in the south and the farmlands in the upstream regions exhibited very low water flow regulation.

As discussed above, the spatial patterns of sediment erosion regulation in scenario 3 for the period July/August were clearly visible (Fig. 8). When comparing the sediment erosion regulation patterns with the land cover/use map, we can see very high sediment erosion regulation in forest areas and wet grasslands in the midstream and downstream regions of the Yanhe river; the upstream regions with terraces and undeveloped shrubland can be assigned to low or very low regulation. The most notable among these is the period of November in all three scenarios, in which the entire river watershed was assigned to classes 4–5. In addition, in March of all three scenarios, no distinction was made in relation to erosion regulation, despite hydrologic differences. In that month, only sub-basin 3 has very low regulation, while all other sub-basins fell into class 5.

Seasonal variation

Monsoon rains in the Yanhe watershed are extremely dominant and result in very high runoff and high sediment transport. As mentioned previously, more than 80% of the annual runoff occurs during summer flooding. Figure A1 shows the simulated monthly mean precipitation over the next 40 years (2021–2060) for the Yan'an meteorological station; more than 70% of the precipitation is concentrated between June and September. However, it shows that annual mean values are not relevant for analyzing water-related questions. For regions with a monsoon climate, such as the Yanhe watershed, it is advisable to conduct seasonal analyses for any land use scenario.

The November period is hydrologically much less important. In November, the Yanhe river enters the dry season or frozen period with few snowfalls. In March, snowmelt recharges the runoff, but the runoff is actually limited. July/August is part of the growing season and is characterized by high evapotranspiration rates. Rainstorm events are frequent, which is an important factor contributing to the large amount of soil erosion in July/August. Water flow regulation was calculated to be low to very high in July/August under all three scenarios but can be assigned to be very low to intermediate for March and November. Erosion regulation was calculated as being low to very high regulation in July/August for all three scenarios. However, due to the class sizes of the relative scale, very high erosion regulation was calculated for all three scenarios, except for sub-basin 7 in scenario 3. In addition, only very low and very high erosion regulations were calculated for all three scenarios (Fig. 8).

Conclusion

In this paper, we developed an integrated model to assess and map the spatial and seasonal effects of future land use changes on ecosystem services. The model results were spatially differentiated among the sub-basins and are depicted after the transformation procedure into a 1–5 relative scale.

Higher regulation services were shown in the lower and middle reaches of the Yanhe river, especially for erosion regulation, due to the high water yield and the low sediment erosion rate. However, lower regulation services were distributed in the upstream areas of the river, especially for erosion regulation, owing to the vegetation interception and serious soil erosion caused by water. Furthermore, seasonal differences can be identified: July/August showed a high water yield and sediment yield, indicating high water flow regulation and low erosion regulation, respectively, but very low water flow regulation and high erosion regulation were calculated for the winter.

Using different land use scenarios, regulation services also showed considerable differences. Scenario 3 had the highest water flow regulation across the entire watershed and the lowest erosion regulation, which were caused by high sediment erosion. Scenario 1 had the highest vegetation coverage and the lowest constructed area of urban land. Meanwhile, the lowest water flow regulation and the highest erosion regulation were calculated. Scenario 2 had intermediate levels of water flow regulation and erosion regulation.

Our research finds that land use changes have great impacts on water yield and sediment yield in the watershed. Excessive urban construction and reckless land reclamation have exacerbated runoff and soil erosion. Increasing vegetation cover in the watershed is conducive to controlling runoff and soil erosion but may also decrease the levels of available water resources.

It is believed that despite the possible limitations and need for certain improvements, the current modeling system provides a reliable approach to simulate and map the impacts of future climate and land use changes on ecosystem services in the Yanhe watershed. Nonetheless, the quantitative study of the influence of model uncertainty on ecosystem services plays a vital role in ecosystem management. The scientific information provided in this study can help decision makers optimize land use in the future, with the goal of strengthening the water-related regulation services delivered by the Yanhe watershed.

Funding information This work was jointly supported by the National Natural Science Foundation of China (grant number 41771198), and the National Natural Science Foundation of China (grant number 41771576).

References

Abbaspour KC, Rouholahnejad E, Vaghefi S, Srinivasan R, Yang H, Kløve B (2015) A continental-scale hydrology and water quality model for Europe: calibration and uncertainty of a high-resolution large-scale SWAT model. J Hydrol 524:733–752

Bellard C, Bertelsmeier C, Leadley P, Thuiller W, Courchamp F (2012) Impacts of climate change on the future of biodiversity. Ecol Lett 15: 365–377

Burkhard B, Kroll F, Nedkov S, Müller F (2012) Mapping ecosystem service supply, demand and budgets. Ecol Indic 21:17–29

Burkhard B, Kandziora M, Hou Y, Müller F (2014) Ecosystem service potentials, flows and demands-concepts for spatial localisation, indication and quantification. Landsc Online 34:1–32

Chen J, Brissette FP, Poulin A, Leconte R (2011) Overall uncertainty study of the hydrological impacts of climate change for a Canadian watershed. Water Resour Res 47:W12509. https://doi.org/10.1029/2011WR010602

Fan M, Shibata H (2015) Simulation of watershed hydrology and stream water quality under land use and climate change scenarios in Teshio River watershed, northern Japan. Ecol Indic 50:79–89

Fu B, Wang S, Su C, Forsius M (2013) Linking ecosystem processes and ecosystem services. Curr Opin Environ Sustain 5:4–10

Hao R, Yu D, Liu Y, Liu Y, Qiao J, Wang X, Du J (2017) Impacts of changes in climate and landscape pattern on ecosystem services. Sci Total Environ 579:718–728

Her Y, Frankenberger J, Chaubey I, Srinivasan R (2015) Threshold effects in HRU definition of the soil and water assessment tool. Trans ASABE 58:367–378

Jacobs S, Burkhard B, Van Daele T, Staes J, Schneiders A (2015) The matrix reloaded': a review of expert knowledge use for mapping ecosystem services. Ecol Model 295:21–30

Jiao Y, Lei H, Yang D, Huang M, Liu D, Yuan X (2017) Impact of vegetation dynamics on hydrological processes in a semi-arid basin by using a land surface-hydrology coupled model. J Hydrol 551: 116–131

Karabulut A, Egoh BN, Lanzanova D, Grizzetti B, Bidoglio G, Pagliero L, Bouraoui F, Aloe A, Reynaud A, Maes J, Vandecasteele I, Mubareka S (2016) Mapping water provisioning services to support the ecosystem–water–food–energy nexus in the Danube river basin. Ecosyst Serv 17:278–292

Leta OT, Nossent J, Velez C, Shrestha NK, van Griensven A, Bauwens W (2015) Assessment of the different sources of uncertainty in a SWAT model of the River Senne (Belgium). Environ Model Softw 68:129–146

Li Z, Fang H (2016) Impacts of climate change on water erosion: a review. Earth Sci Rev 163:94–117

Li J, Zhou ZX (2015) Coupled analysis on landscape pattern and hydrological processes in Yanhe watershed of China. Sci Total Environ 505:927–938

Liao Y, Gao G, Xie Y (2009) Impacts of climate changes on parameters of a weather generator for daily precipitation in China. Acta Geograph Sin 64:871–878

Liao Y, Chen D, Xie Y (2013) Spatial variability of the parameters of the Chinese stochastic weather generator for daily non-precipitation variables simulation in China. Acta Meteorol Sin 71:1103–1114

Lin L, Sills E, Cheshire H (2014) Targeting areas for reducing emissions from deforestation and forest degradation (REDD+) projects in Tanzania. Glob Environ Chang 24:277–286

Lin B, Chen X, Yao H, Chen Y, Liu M, Gao L, James A (2015) Analyses of landuse change impacts on catchment runoff using different time indicators based on SWAT model. Ecol Indic 58:55–63

Luo Y, Yang ST, Zhao CS, Liu XY, Liu CM, Wu LN, Zhao HG, Zhang YC (2014) The effect of environmental factors on spatial variability in land use change in the high-sediment region of China's loess plateau. J Geogr Sci 24:802–814

Meaurio M, Zabaleta A, Uriarte JA, Srinivasan R, Antigüedad I (2015) Evaluation of SWAT models performance to simulate streamflow spatial origin. The case of a small forested watershed. J Hydrol 525:326–334

Neitsch SL, Arnold JG, Kiniry JR, Williams JR (2011) Soil and water assessment tool theoretical documentation version 2009. Texas Water Resources Institute, College Station

Ning J, Gao Z, Lu Q (2015) Runoff simulation using a modified SWAT model with spatially continuous HRUs. Environ Earth Sci 74:5895–5905

Panagopoulos Y, Gassman PW, Arritt RW, Herzmann DE, Campbell TD, Jha MK, Kling CL, Srinivasan R, White M, Arnold JG (2014) Surface water quality and cropping systems sustainability under a changing climate in the Upper Mississippi River Basin. J Soil Water Conserv 69:483–494

Panagopoulos Y, Gassman PW, Jha MK, Kling CL, Campbell T, Srinivasan R, White M, Arnold JG (2015) A refined regional modeling approach for the Corn Belt—experiences and recommendations for large-scale integrated modeling. J Hydrol 524:348–366

Peng J, Liu Y, Liu Z, Yang Y (2017) Mapping spatial non-stationarity of human-natural factors associated with agricultural landscape multifunctionality in Beijing–Tianjin–Hebei region, China. Agric Ecosyst Environ 246:221–233

Pérez-Vega A, Mas J-F, Ligmann-Zielinska A (2012) Comparing two approaches to land use/cover change modeling and their implications for the assessment of biodiversity loss in a deciduous tropical forest. Environ Model Softw 29:11–23

Pervez MS, Henebry GM (2015) Assessing the impacts of climate and land use and land cover change on the freshwater availability in the Brahmaputra River basin. J Hydrol: Reg Stud 3:285–311

Pontius RG Jr, Schneider LC (2001) Land-cover change model validation by an ROC method for the Ipswich watershed, Massachusetts, USA. Agric Ecosyst Environ 85:239–248

Pullanikkatil D, Palamuleni LG, Ruhiiga TM (2016) Land use/land cover change and implications for ecosystems services in the Likangala River Catchment, Malawi. Phys Chem Earth Parts A/B/C 93:96–103

Qiu L-J, Zheng F-L, Yin R-S (2012) SWAT-based runoff and sediment simulation in a small watershed, the loessial hilly-gullied region of China: capabilities and challenges. Int J Sediment Res 27:226–234

Quintas-Soriano C, Castro AJ, Castro H, García-Llorente M (2016) Impacts of land use change on ecosystem services and implications for human well-being in Spanish drylands. Land Use Policy 54:534–548

Rasul G (2016) Managing the food, water, and energy nexus for achieving the Sustainable Development Goals in South Asia. Environ Dev 18:14–25

Schmalz B, Kruse M, Kiesel J, Müller F, Fohrer N (2016) Water-related ecosystem services in western Siberian lowland basins—analysing and mapping spatial and seasonal effects on regulating services based on ecohydrological modelling results. Ecol Indic 71:55–65

Shrestha MK, Recknagel F, Frizenschaf J, Meyer W (2017) Future climate and land uses effects on flow and nutrient loads of a Mediterranean catchment in South Australia. Sci Total Environ 590-591:186–193

Strauch M, Bernhofer C, Koide S, Volk M, Lorz C, Makeschin F (2012) Using precipitation data ensemble for uncertainty analysis in SWAT streamflow simulation. J Hydrol 414-415:413–424

Sun WY, Shao QQ, Liu JY, Zhai J (2014) Assessing the effects of land use and topography on soil erosion on the loess plateau in China. Catena 121:151–163

Tan ML, Ficklin DL, Dixon B, Ibrahim AL, Yusop Z, Chaplot V (2015) Impacts of DEM resolution, source, and resampling technique on SWAT-simulated streamflow. Appl Geogr 63:357–368

Uniyal B, Jha MK, Verma AK (2015) Assessing climate change impact on water balance components of a river basin using SWAT model. Water Resour Manag 29:4767–4785

Vigerstol KL, Aukema JE (2011) A comparison of tools for modeling freshwater ecosystem services. J Environ Manag 92:2403–2409

van Vliet J, Bregt AK, Brown DG, van Delden H, Heckbert S, Verburg PH (2016) A review of current calibration and validation practices in land-change modeling. Environ Model Softw 82:174–182

Wang S, Fu B, Piao S, Lü Y, Ciais P, Feng X, Wang Y (2015) Reduced sediment transport in the Yellow River due to anthropogenic changes. Nat Geosci 9:38–41

Williams JR, Arnold JG (1997) A system of erosion—sediment yield models. Soil Technol 11:43–55

Wilson CO, Weng Q (2011) Simulating the impacts of future land use and climate changes on surface water quality in the Des Plaines River watershed, Chicago Metropolitan Statistical Area, Illinois. Sci Total Environ 409:4387–4405

Woldemeskel FM, Sharma A, Sivakumar B, Mehrotra R (2012) An error estimation method for precipitation and temperature projections for future climates. J Geophys Res Atmos 117:1–13. https://doi.org/10.1029/2012jd018062

Wu C-F, Lin Y-P, Chiang L-C, Huang T (2014) Assessing highway's impacts on landscape patterns and ecosystem services: a case study in Puli Township, Taiwan. Landsc Urban Plan 128:60–71

Xu F, Dong G, Wang Q, Liu L, Yu W, Men C, Liu R (2016) Impacts of DEM uncertainties on critical source areas identification for non-point source pollution control based on SWAT model. J Hydrol 540:355–367

Yan R, Zhang X, Yan S, Zhang J, Chen H (2017) Spatial patterns of hydrological responses to land use/cover change in a catchment on the loess plateau, China. Ecol Indic. https://doi.org/10.1016/j.ecolind.2017.04.013

Yang X, Zheng X-Q, Chen R (2014) A land use change model: integrating landscape pattern indexes and Markov-CA. Ecol Model 283:1–7

Yesuf HM, Assen M, Alamirew T, Melesse AM (2015) Modeling of sediment yield in Maybar gauged watershed using SWAT, northeast Ethiopia. Catena 127:191–205

Zhang P, Liu R, Bao Y, Wang J, Yu W, Shen Z (2014a) Uncertainty of SWAT model at different DEM resolutions in a large mountainous watershed. Water Res 53:132–144

Zhang X, Y-P X, Fu G (2014b) Uncertainties in SWAT extreme flow simulation under climate change. J Hydrol 515:205–222

Zhang D, Chen X, Yao H, Lin B (2015) Improved calibration scheme of SWAT by separating wet and dry seasons. Ecol Model 301:54–61

Zhao G, Liu J, Kuang W, Ouyang Z, Xie Z (2015) Disturbance impacts of land use change on biodiversity conservation priority areas across China: 1990–2010. J Geogr Sci 25:515–529

Zhou ZX, Li J (2015) The correlation analysis on the landscape pattern index and hydrological processes in the Yanhe watershed, China. J Hydrol 524:417–426

Zuo D, Xu Z, Yao W, Jin S, Xiao P, Ran D (2016) Assessing the effects of changes in land use and climate on runoff and sediment yields from a watershed in the loess plateau of China. Sci Total Environ 544: 238–250